Journal of Environmental Management 196 (2017) 466–475

Contents lists available at ScienceDirect

Journal of Environmental Management

journal homepage: www.elsevier.com/locate/jenvman

Research article

# Evaluation of heavy crude oil from a water-oil model system as starting material for the preparation of adsorbents type NaY zeolite-templated carbon

Cindy J. Elles-Pérez [a], Amner Muñoz-Acevedo [b], Andrés Guzmán [a, *], Hernando Camargo [c], José Henao [d]

[a] Department of Civil and Environmental Engineering, Universidad del Norte, km 5 via Pto. Colombia, P.O. Box 1569-51820, Barranquilla, Atlántico, Colombia
[b] Department of Chemistry and Biology, Universidad del Norte, km 5 via Pto. Colombia, P.O. Box 1569-51820, Barranquilla, Atlántico, Colombia
[c] Faculty of Environmental Chemistry, Universidad Santo Tomás sede Bucaramanga, Cr 18 #9-27, Bucaramanga, Santander, Colombia
[d] School of Chemistry, Universidad Industrial de Santander, Cr 27 Cl 9, Bucaramanga, Santander, Colombia

ARTICLE INFO

*Article history:*
Received 10 November 2016
Received in revised form
5 March 2017
Accepted 16 March 2017

*Keywords:*
Mesoporous carbons
ZTC materials
Heavy oil
NaY zeolite
Oil-water model

ABSTRACT

In this work, NaY zeolite is explored as a possible "template" to obtain porous materials type ZTC from the adsorption of heavy crude oil in a water-oil model system (emulsion). In order to produce the adsorbents, a cationic surfactant is selected to facilitate the adsorption of the crude oil into the pores of the zeolite and to get the composite, which was activated with controlled thermal treatments (T: 700 −800 °C and t: 0.5−1 h) in inert conditions ($N_2$ gaseous). The starting materials, composite and porous carbons were characterized using structural/surface analysis techniques (API Gravity, SARA, IR, XRD, XRF, TGA, Langmuir isotherms, BET and SEM). The results showed that four types of mesoporous carbons were produced with specific surface areas between 70 ± 1 $m^2/g$ and 220 ± 3 $m^2/g$, average pore volumes between 0.144 $cm^3/g$ and 0.40 $cm^3/g$ and average pore widths between 4.9 nm and 8.3 nm. The activation conditions of 800 °C and 1 h allowed to make the carbonaceous material with the best surface characteristics (220 ± 3 $m^2/g$, 0.27 $cm^3/g$, and 4.9 nm). Therefore, it is concluded that under assay conditions employed, the heavy crude oil, as a mixed model (water-oil), from an aqueous environment is a starting material suitable for preparation of "mesoporous" carbons.



## 1. Introduction

The oil industry has been of great importance for being one of the main sources of energy production and in the world, daily *ca.* 93.7 million barrels are consumed (US. Energy Information Administration, 2016). However, this industry has been affected by accidents that have caused some oil spills and environmental disasters (1970–2015); during this period more than 40 million barrels of oil were spilled into the sea (ITOPF, 2015). Reports of accidents in the last decades includes clogging of the Exxon Valdez boat on the coasts of Alaska (Fukuyama et al., 2014), the explosion and sinking of the Deepwater Horizon oil rig in the Gulf of Mexico (Wei et al., 2012), and the leaks in the Bohai Bay platforms (China) (Liu and Zhu, 2014). Since 1986 in Colombia, *ca.* 4 million barrels of oil have been spilled because of accidents and attacks against the oil infrastructure (MINAMBIENTE, 2015). These accidents have resulted in significant economic, ecological and environmental damages at different levels (poisoning, reproductive problems, and death) on the aquatic and terrestrial biota of the surrounding areas. According to Kingston (2002), these unfavourable effects could appear in the short, mid and long-term (up to 10 years) after the environmental incident has occurred.

In the oil industry, the contingency plans that have been available to mitigate the damages and the side effects when a spill occurs on different "sources" (water/sediment/soil), include methods such as biological remediation (Ron and Rosenberg, 2014), membrane filtration (Tansel et al., 1995), dispersion (Riehm et al., 2015) and adsorption (Raj and Joy, 2015). The last method is the preferred alternative due to its high efficiency, easy handling, and

* Corresponding author.
*E-mail addresses:* cindyelles@gmail.com (C.J. Elles-Pérez), amnerm@uninorte.edu.co (A. Muñoz-Acevedo), faguzman@uninorte.edu.co (A. Guzmán), director@ginmea.org (H. Camargo), jahenao@uis.edu.co (J. Henao).

http://dx.doi.org/10.1016/j.jenvman.2017.03.049
0301-4797/

affordability. Some industries have been focused on the use of porous materials (zeolites, activated carbons, diatomaceous earth, etc.) for the treatment of contaminated water (Al-Majed et al., 2012; Jovanovic et al., 2014; Mohanty et al., 2005). Nonetheless, once the adsorption process is carried out on the spill and the pores of the adsorbent are saturated, a "waste (composite)" is produced which does not have any kind of exploitation/application in the present but rather is disposed or incinerated (Li et al., 2015).

The waste or composite could be exploited to produce new porous materials called zeolite-templated carbons (ZTC), if the adsorbent used is a zeolite. This would have a positive environmental impact, reducing the disposal problems associated to the large quantities of adsorbent used for oil clean-up.

ZTC are materials obtained in the inner cavities of the zeolite with the aim to replicate the pore-structural regularity of the zeolite framework by loading a carbon precursor (Radovic, 2007). According to the revised scientific literature, some ZTC materials have been synthesized by adsorption of organic compounds with different structural characteristics such as furfuryl alcohol (Kyotani et al., 1997, 2003; Ma et al., 2002), acrylonitrile, vinyl acetate, pyrene, etc. (Meyers et al., 2001), on zeolites (Y, β, ZSM-5) templates by using the impregnation method (liquid phase).

The majority of ZTC produced had as main characteristic a high surface development (245 $m^2/g$–3683 $m^2/g$) related to micropore structures (Kyotani et al., 1997; Meyers et al., 2001; Ma et al., 2002; Kyotani et al., 2003). Gierszal et al. (2005) investigated the use of mesophase and petroleum pitches as carbon precursors for the development of ordered mesoporous carbons, however they use alcoholic solvents and increased temperature process to achieve the adsorption of the carbon into the template, so the use of a crude oil from a water system (composite) has not yet been reported as a ZTC precursor.

In this work, the potential use of heavy crude oil is evaluated from a water-oil model system as a starting material or carbon precursor to obtain some zeolite template carbons (ZTC).

## 2. Materials and methods

### 2.1. Reagents and materials

The following reagents and materials are present in this research: n-pentane (95%, Carlo Erba), dichloromethane (95%, J.T. Baker), toluene (95%, BDH), hexadecyltrimethylammonium bromide (HDTMA-Br, 99%, Sigma-Aldrich), methylthioninium chloride (methylene blue dye, Carlo Erba), HCl (37%, Merck), NaOH (99%, Merck), NaY Zeolite (CBV100, Zeolist), and heavy crude oil (provided by *Atlantic Oils Terminal*, Barranquilla, Colombia).

### 2.2. Adsorption of heavy crude oil on NaY zeolite

In order to prepare the water-crude oil model system, it is followed the procedure described by Jin et al. (2008), mixing the heavy oil (0.1 g), the cationic surfactant HDTMA-Br (2%) and distilled water (50 mL) within an Erlenmeyer flask. The emulsion formed required a stirring process of 24 h at 200 rpm.

The adsorption of crude oil on Z-NaY was made by the impregnation method as proposed by Su et al. (2004) with some modifications. The zeolite (1 g, preconditioned at 120 °C, 12 h) was added after the stabilization of the emulsion (24 h); then, the whole system was stirred for 24 h at 300 rpm. The resulting solid (composite Z-NaY/crude oil) was separated by filtration and dried in a conventional oven (100 °C, 24 h).

**Table 1**
SARA analysis for heavy crude oil.

| Fraction | Weight, % |
|---|---|
| Saturate | 38.7 ± 0.3 |
| Aromatic | 44 ± 1 |
| Resin | 6.4 ± 0.1 |
| Asphaltene | 10.9 ± 0.2 |

### 2.3. Activation of the composite Z-NaY/crude oil

The activation of the composite obtained was carried out using different temperatures (700–800 °C, Nabertherm Furnace N41H) and time treatments (0.5–1 h), in inert conditions ($N_2$, constant flow), according to the method disclosed by Ma et al. (2002). As a result, four carbonaceous materials were produced, which were washed to remove the zeolite (50% NaOH, hot water), filtrated, dried (120 °C, 6 h), and characterized by structural/surface analysis techniques.

### 2.4. Structural/surface characterization

The sample of crude oil was characterized through the API gravity (hydrometer method) and SARA (saturates, aromatics, resins, asphaltenes) physicochemical analysis, based on the ASTM D1298 - 12b (ASTM International, 2012) and ASTM D2007 - 11 (ASTM International, 2016).

The identification of the crystalline phases and elemental analysis of the Z-NaY was carried out by X-ray diffraction of polycrystalline samples (powder X-ray diffractometer with DaVinci design, D8 Advance model, Bruker) and X-ray fluorescence (wavelength dispersive X-ray fluorescence spectrometer, S8 Tiger 4 kW model, Bruker), respectively. The chemical groups of the Z-NaY and the adsorbents ZTC were determined by Fourier transform infrared spectroscopy (IRAffinity-1S FTIR spectrophotometer, Shimadzu).

There are different methods for monitoring precursor adsorption process in the literature (Bandura et al., 2015; Karakasi and Moutsatsou, 2010; Sakthivel et al., 2013). The method adopted in this research for a general adsorption process description was thermogravimetric analysis (TGA, Q500 analyzer, T.A. Instruments) due to its accessibility and availability. The composite was analysed under an inert atmosphere and with a heating rate of 10 °C/min, from 25 °C to 800 °C.

Surface analysis of the Z-NaY and the carbons was conducted by scanning electron microscopy (SEM, JSM 6490 LV microscope, Jeol) and the BET method (ASAP 2020 analyzer, Micromeritics; liquid $N_2$, 77 K, and relative P: 0.01–0.30). Pore size distribution was determined with Barrett-Joyner-Halenda (BJH) method.

## 3. Results and discussion

### 3.1. Physicochemical characterization of crude oil

The API gravity value of 12.3° determined for the crude oil, allowed us to establish that it was a heavy oil (Speight, 2014). According to SARA analysis, the crude oil was constituted mainly by aromatic and saturated compounds (Table 1).

**Table 2**
Crystal structures for the NaY zeolite by XRD.

| Phase | | Name | PDF No |
|---|---|---|---|
| Crystallines | $Na_2\ Al_2\ Si_{4.5}\ O_{13}\ x\ H_2O$ | Faujasite | 000-43-0168 |
| | $Na_{0.931}\ (Al\ Si_2\ O_6)\ (H_2O)$ | Analcime | 010-89-6324 |

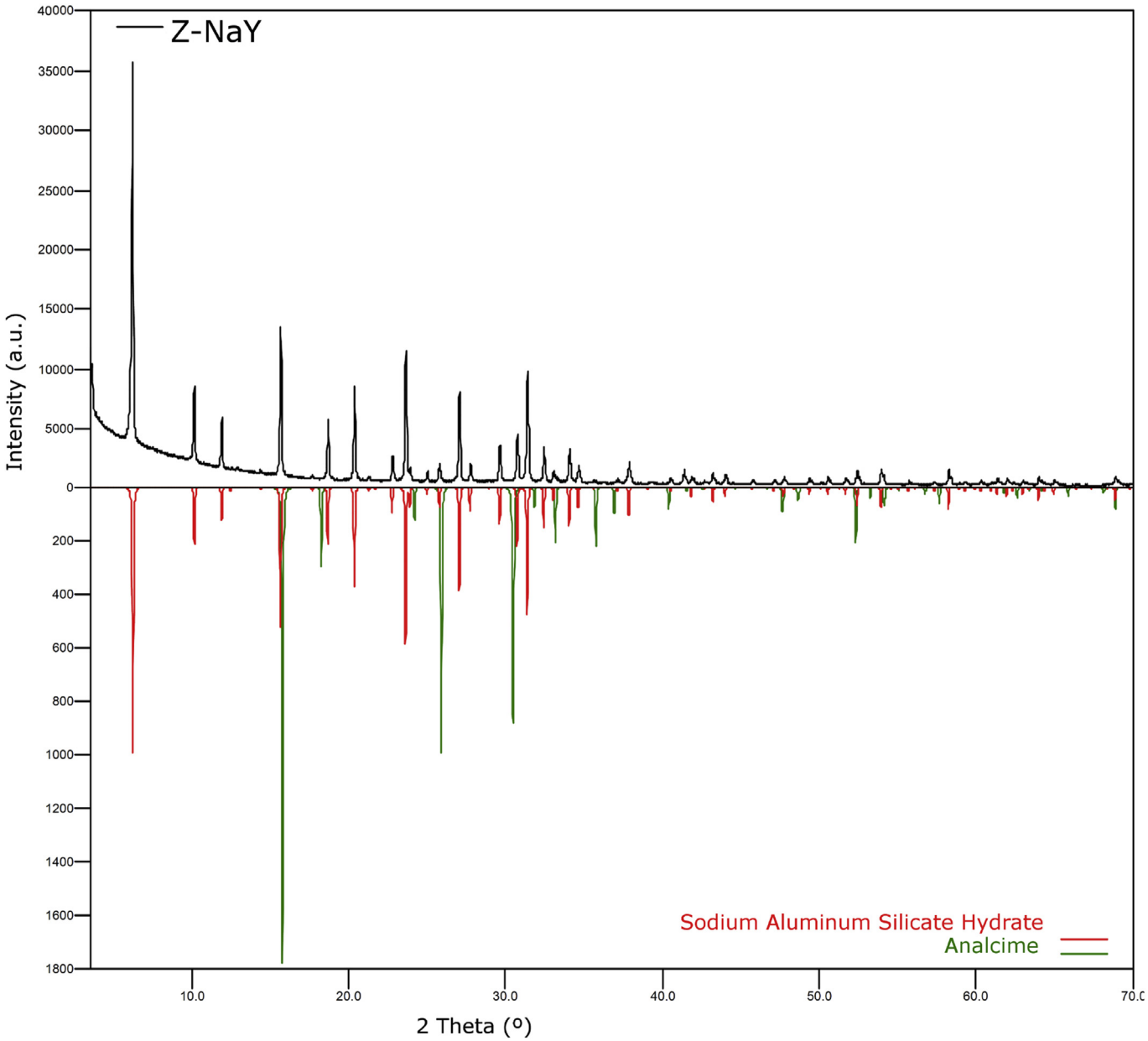


**Fig. 1.** Comparison of the diffraction profiles of Z-NaY and the crystalline phases identified (Faujasite y Analcime).

### 3.2. X-ray diffraction analysis of Z-NaY

Qualitative analysis by means of XRD of polycrystalline samples allowed to identify the faujasite (majority phase) and the analcime (Table 2) as the main crystalline phases of Z-NaY. Fig. 1 shows the comparison between the diffraction profiles of the zeolite of interest and the crystalline phases found and reported in the PDF-2 database of the International Centre for Diffraction Data (PDF-2, ICDD).

### 3.3. Elemental analysis by X-ray fluorescence of Z-NaY

The elemental composition of the NaY zeolite by XRF, represented in the form of oxides, is shown in Table 3. The main components found were $SiO_2$, $Al_2O_3$, and $Na_2O$, which are the characteristic constituents of a synthetic NaY zeolite (Zeolyst, n.d.).

**Table 3**
Elemental composition for NaY zeolite by XRF.

| Constituent | Amount (%) |
|---|---|
| $SiO_2$ | 65.1 ± 0.1 |
| $Al_2O_3$ | 22.10 ± 0.08 |
| $Na_2O$ | 12.5 ± 0.2 |
| CaO | 0.158 ± 0.004 |
| $SO_3$ | 0.078 ± 0.006 |
| $K_2O$ | 0.028 ± 0.004 |
| $Fe_2O_3$ | 0.025 ± 0.001 |
| $TiO_2$ | 0.025 ± 0.003 |
| CuO | 0.007 ± 0.001 |
| $ZrO_2$ | 0.001 ± 0.000 |

### 3.4. Infrared analysis of Z-NaY

The infrared spectrum of the NaY zeolite (Fig. 2), displays the characteristic absorption bands at 569 $cm^{-1}$, 785 $cm^{-1}$, 989 $cm^{-1}$ and 3417 $cm^{-1}$. These bands can be caused by the tetrahedral

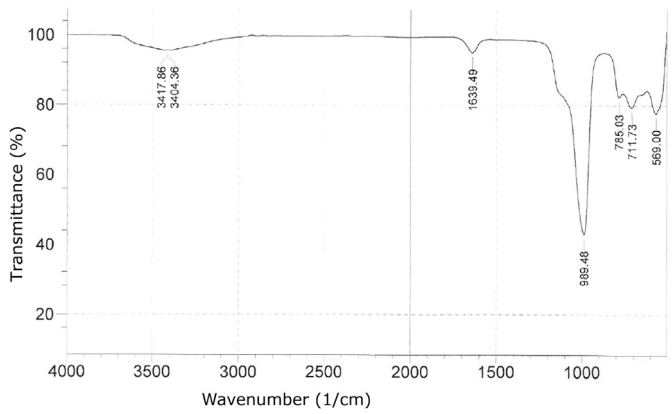


**Fig. 2.** Infrared spectrum of Z-NaY.

vibrations related to the rings (characteristic of faujasite), to the M-O vibrations (M: Si, Al) and to the OH groups linked to $Na^+$ ion, respectively (Li, 2005; Sang et al., 2006).

### 3.5. Scanning electron microscopy of the composite Z-NaY/crude oil

The Z-NaY and the composite were analysed by scanning electron microscopy to assure the adsorption process of crude oil. Fig. 3 shows a comparison of these images. The composite (Fig. 3b) showed a higher surface density than the unmodified zeolite (Fig. 3a) as a result of pore filling. Furthermore, the crystals in the composite are bigger and less sharp, and its surface is smoother than the zeolite crystals. This could be associated with adsorption process of the oil that took place on the zeolite surface.

### 3.6. Thermogravimetric analysis of the composite

A thermogravimetric analysis was performed to the composite in order to determine and correlate the weight losses and changes, during the activation process, with the final characteristics of the adsorbent materials.

The TGA analysis provided the weight loss profile during the activation process of the composite (Fig. 4). The global weight loss calculated by this technique results in 30.2%. Based on the derivative weight loss curve, three maximum peaks were found at temperatures of 99.8 °C, 234.0 °C, and 397.5 °C with weight losses of 19.9%, 1.8%, and 8.5%, respectively. These losses could be correlated with the presence of water, volatile matter adsorbed on the surface of the sample, hydration/crystallization water existing in the material and re-polymerization of the carbonaceous structure (Tiwari and Deo, 2012). The last two peaks corresponding to 10.3% of weight loss could be attributed to the total crude oil loaded in the zeolite surface (for 1 g of the composite, 0.1 g corresponds to the carbon loaded).

### 3.7. Adsorption/desorption and specific surface analysis of the NaY zeolite-templated carbon

ZTC materials were labelled according to the activation conditions (T: 700 °C −800 °C, A: 0.5 h, B: 1 h) as follows: ZTC700A, ZTC700B, ZTC800A, ZTC800B.

Langmuir isotherms were obtained from the data of adsorption of nitrogen at 77 K to carry out the adsorption/desorption analysis of the different porous materials. Fig. 5 presents the isotherms depicted for each evaluated adsorbents. The isotherm of the NaY zeolite was type I, which in agreement with the IUPAC (Thommes et al., 2015) is a distinguished feature of the microporous materials. Meanwhile the four ZTC materials exhibited type IV isotherms with desorption hysteresis H4 (feature for mesoporous carbons), which could be explained by the capillary condensation that occurs

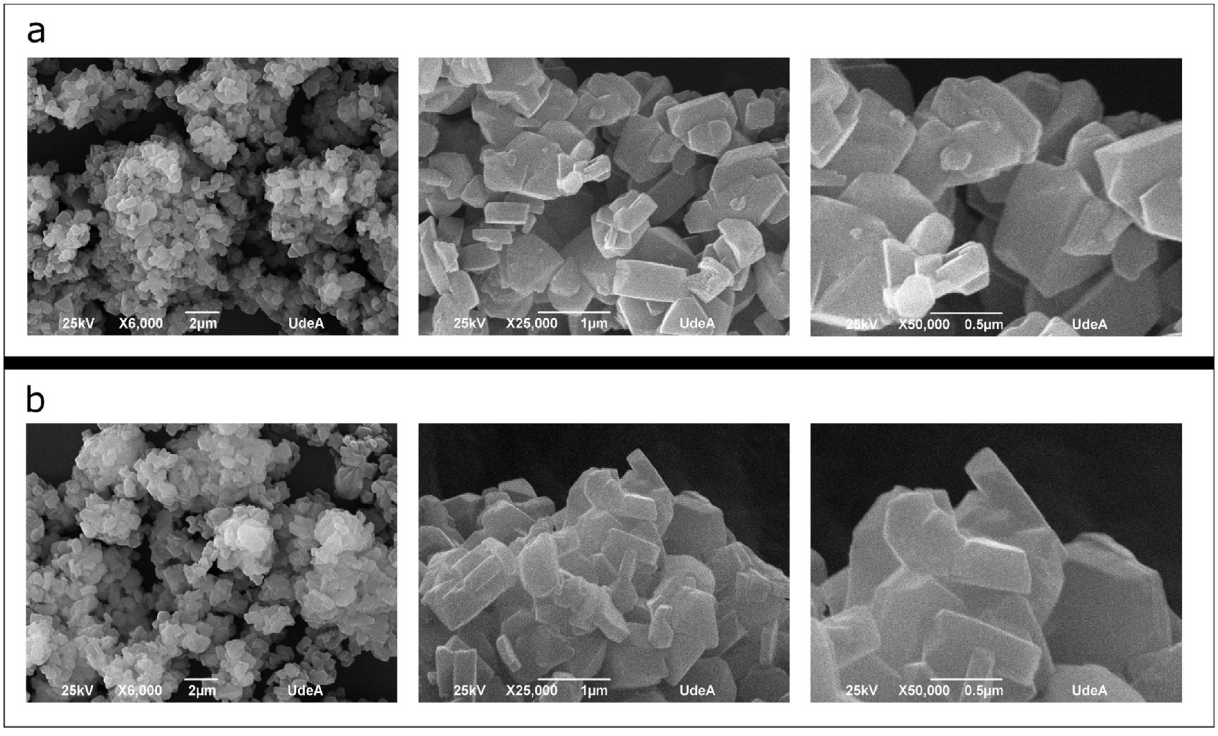


**Fig. 3.** SEM images (2 µm, ×6000; 1 µm, ×25000; 0.5 µm, ×50000) for **a.** Z-NaY and **b.** Composite Z-NaY/crude oil.

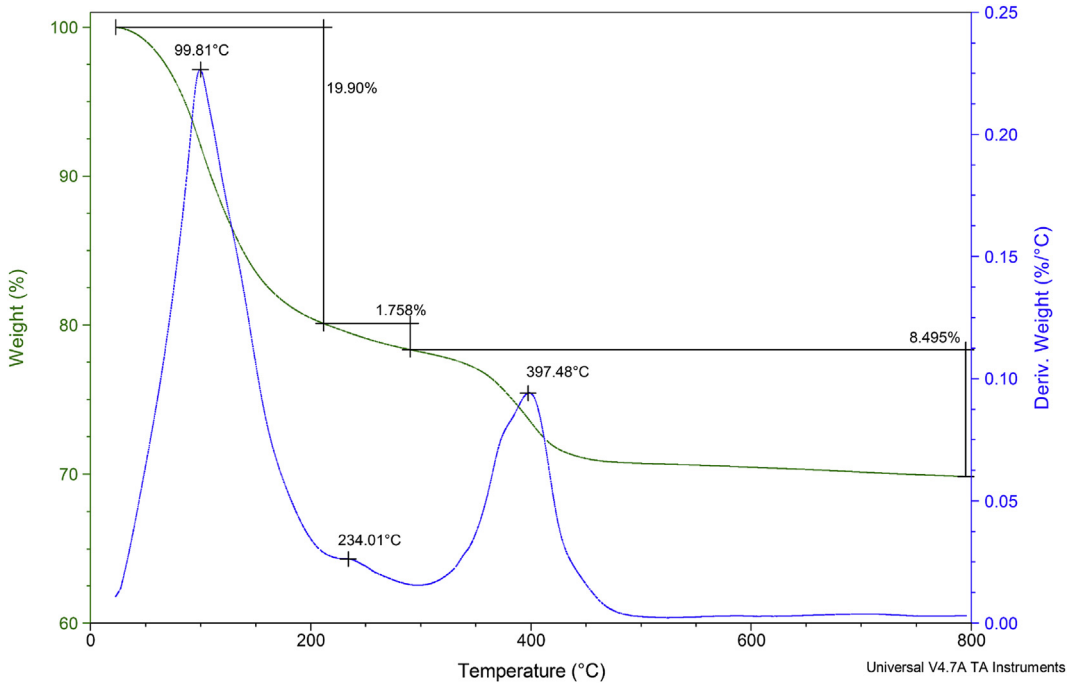


**Fig. 4.** Weight loss profile (including derivatives) for the composite Z-NaY/crude oil during the activation process by TGA analysis.

in the mesopores, the ZTC800B exhibited the maximum uptake of nitrogen at low relative pressure, corresponding to the presence of some micropores. Ma et al. (2002) also found a hysteresis loop for ZTC using furfuryl alcohol; nevertheless, the results of these $N_2$ adsorption isotherms showed that the structures were predominantly microporous.

The comparison of the isotherms of the carbons obtained at 700 °C and 800 °C showed significant differences in adsorption, highlighting the essential role of the temperature and time on the surface development. It means that at a higher activation temperature and time, the adsorption capacity of the ZTC adsorbents increased.

The BET surface analysis confirmed the effects of temperature and time on the activation of the porous materials (Table 4); therefore, the carbons obtained at 800 °C had the highest specific surface areas, and at this temperature, the

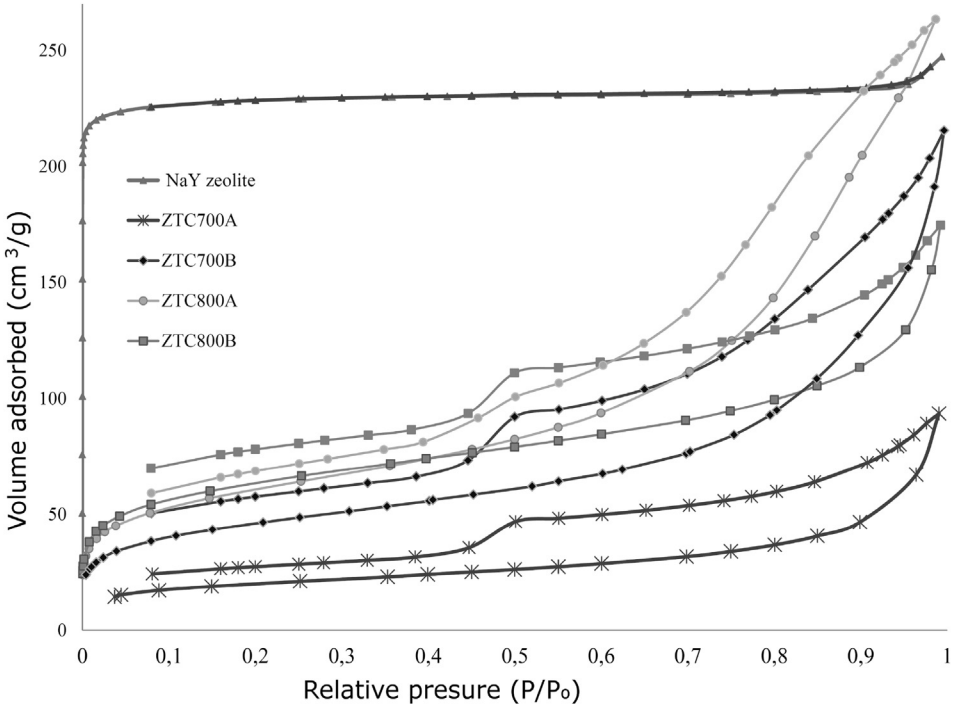


**Fig. 5.** Adsorption/desorption isotherms for the NaY zeolite and the ZTC materials.

**Table 4**
Specific surface area, average pore width, average particle size values determined by BET analysis and pore volume by single point adsorption.

| Parameter | Sample | | | | |
|---|---|---|---|---|---|
| | Z-NaY | ZTC700A | ZTC700B | ZTC800A | ZTC800B |
| $S_{BET}$ ($m^2$/g) | 736 | 70 | 161 | 212 | 220 |
| $V_t$[a] ($cm^3$/g) | 0.382 | 0.144 | 0.333 | 0.407 | 0.270 |
| APW[b] (nm) | 2.1 | 8.3 | 8.2 | 7.7 | 4.9 |
| APS[c] (nm) | 8.2 | 85.8 | 37.1 | 28.2 | 27.4 |

[a] Vt – *Total pore volume*.
[b] APW – *Average Pore Width*.
[c] APS – *Average Particle Size*.

porous materials activated for 1 h reached the smallest average pore width.

Meyers et al.(2001) obtained ZTC with surface areas in the ranges of 245 $m^2$/g –947 $m^2$/g using compounds of lower molecular weight (furfuryl alcohol, vinyl acetate, and acrylonitrile), which are higher that the ZTC obtained in this work. This discrepancy can be ascribed to the adsorption of the crude oil on the Z-NaY: during the adsorption stage, due to the molecular diversity of heavy oil, the medium-high weight compounds could not penetrate completely the pores of the zeolite or could have obstructed the inlet for lighter molecules. On the other hand, Meyers et al. used a high molecular weight compound as pyrene, then the surface areas were between 2.1 $m^2$/g–35 $m^2$/g (Meyers et al., 2001). Comparing these results with the carbons obtained in the present work with heavy oil (70 $m^2$/g–220 $m^2$/g) there is an improvement (35 $m^2$/g vs 220 $m^2$/g) in the porosity development of the carbons using the impregnation method. The use of the surfactant HDTMA-Br might have improved the uptake of the organic compounds in the zeolite pores as it was previously reported by Vidal et al. (2012).

The pore size distributions of the materials were determined by the Barrett-Joyner-Halenda (BJH) method. The comparison between ZTC800A, B carbons and Z-NaY is exposed in Fig. 6.

The ZTC800A and ZTC800B both exhibited a typical distribution for mesoporous carbons. However, there were differences in the

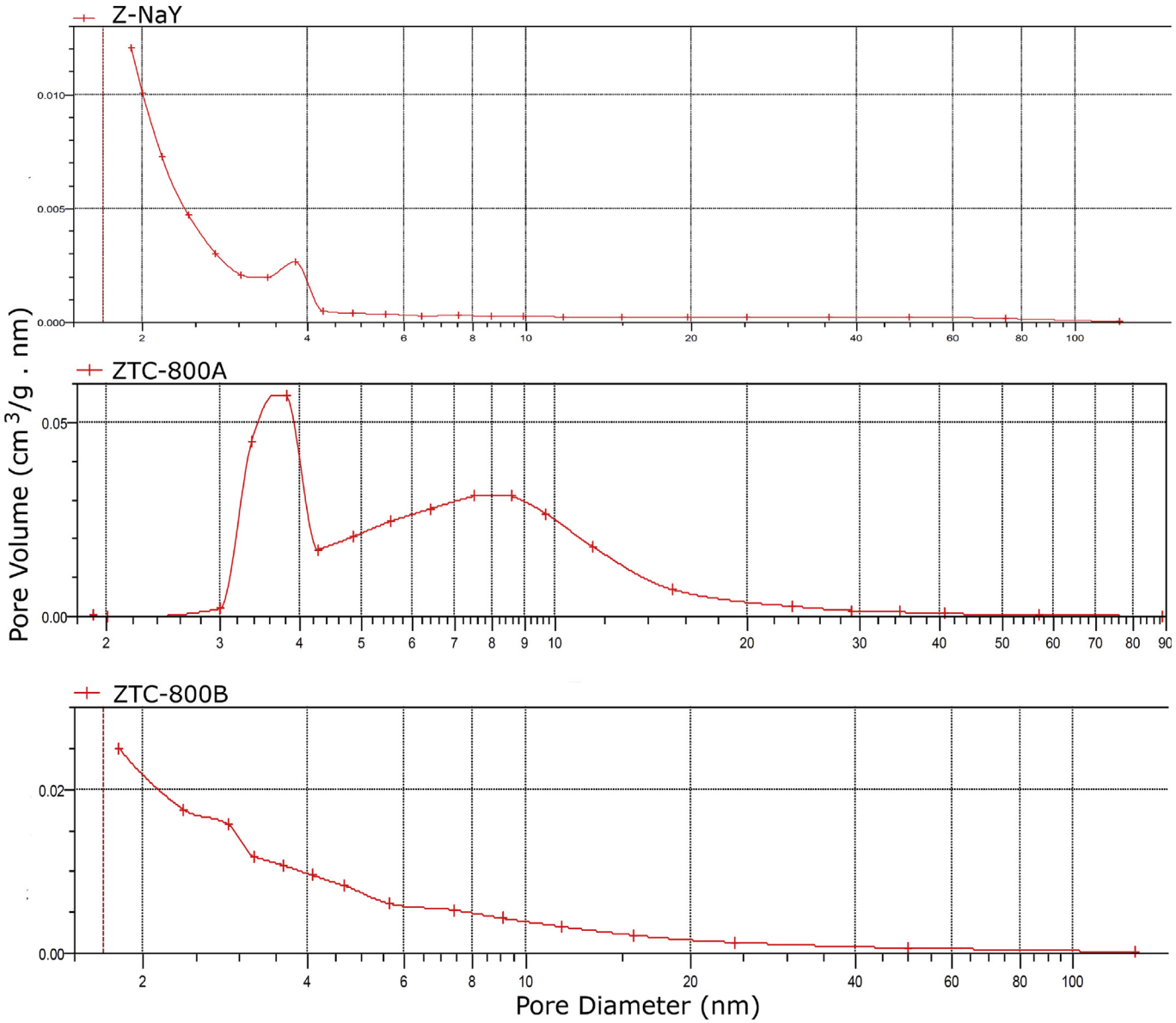


**Fig. 6.** Pore size distributions for the ZTC800A,B materials and Z-NaY by Barrett-Joyner-Halenda method (Harkins and Jura – Faas Correction).

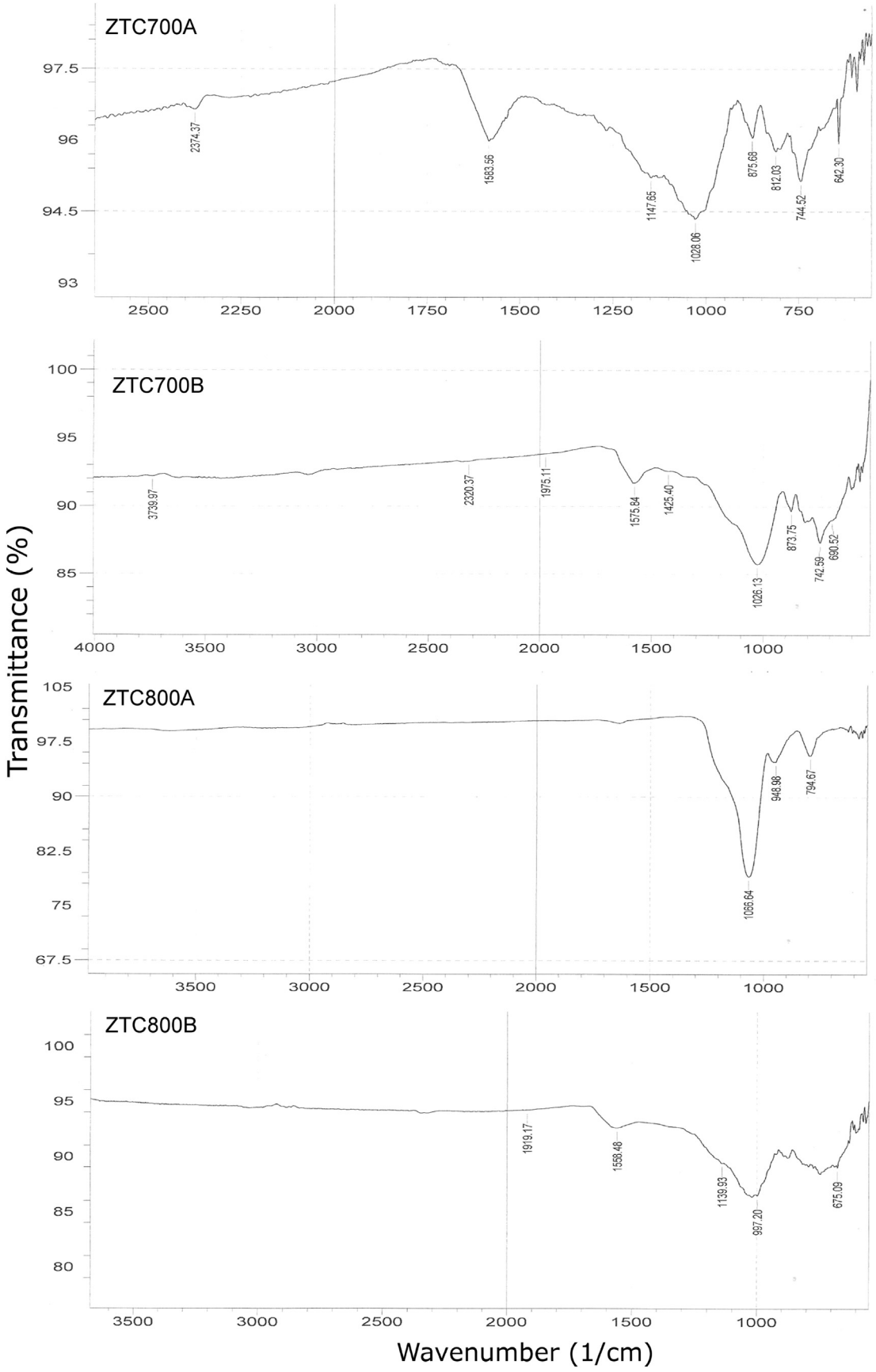


**Fig. 7.** Infrared spectra for the ZTC materials.

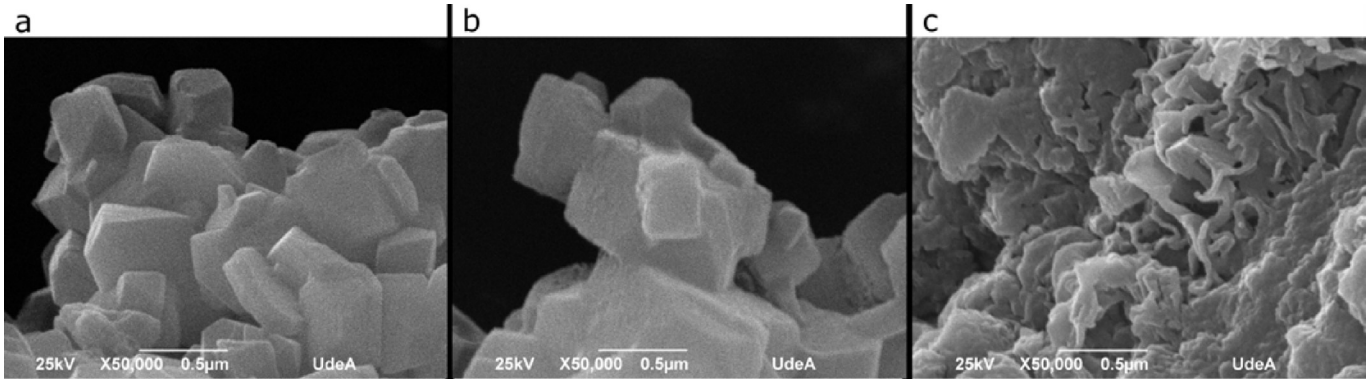


**Fig. 8.** SEM images (500 nm, ×50000) for **a.** Z-NaY, **b**. Composite, **c**. ZTC800B.

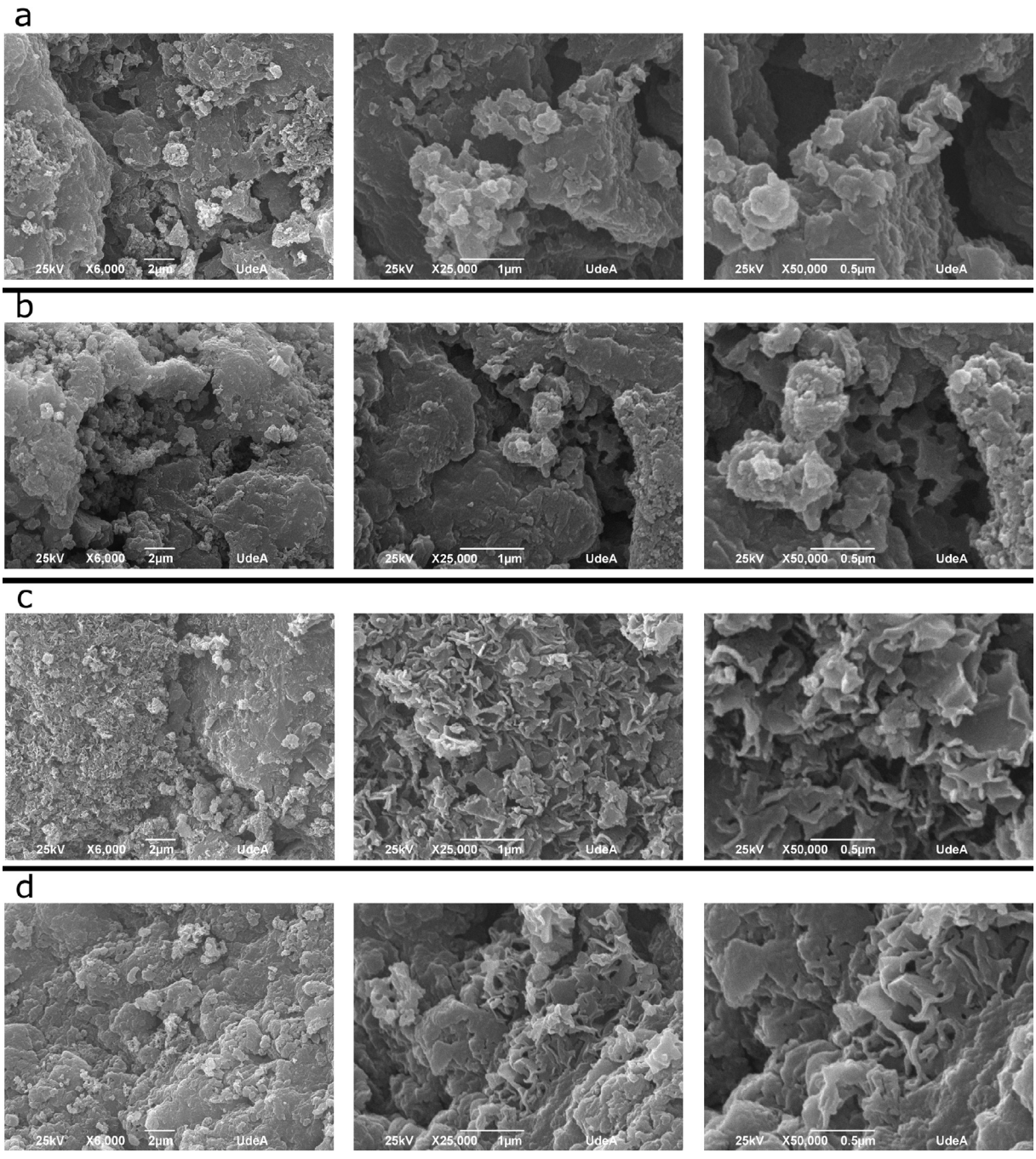


**Fig. 9.** SEM images (2 μm, ×6000; 1 μm, ×25000; 0.5 μm, ×50000) for ZTC materials **a.**700A, **b**.700B, **c**. 800A, and **d.** 800B.

pore sizes of each one of these materials: ZTC800A showed mainly mesopores with pore sizes between 3 nm and 40 nm, with some pores larger than 40 nm; whereas ZTC800B had pore sizes between 2 nm and 60 nm, with microporosities (pore less than 2 nm).

### 3.8. Infrared analysis of the ZTC

Fig. 7 shows the spectra acquired by IR spectroscopy for the four carbonized samples. The characteristic absorption bands were located between 640 $cm^{-1}$ and 1590 $cm^{-1}$. Therefore, the highest absorption bands were encompassed between 997 $cm^{-1}$ and 1066 $cm^{-1}$, attributed to the C–O stretching and vibrations (ether group) (Conley, 1979; Marsh and Rodríguez-Reinoso, 2006); whereas the bands found between 1560 $cm^{-1}$ and 1590 $cm^{-1}$ can be associated to stretching and vibrations of unconjugated carbonyl groups and aromatic systems (Bansal and Goyal, 2005; Conley, 1979). Finally, the bands presented between 650 $cm^{-1}$ and 880 $cm^{-1}$, apparently come from an asymmetric twisting out of the plane of the C–H bonds (Al-Qodah and Shawabkah, 2009), representatives of the hydrocarbon structures.

### 3.9. Scanning electron microscopy of the ZTC

Fig. 8 shows a comparison of the Z-NaY, the composite and the ZTC800B. The ZTC materials synthesized at different conditions developed an amorphous structure compared to the crystalline structure of the NaY zeolite. Meyers et al. (2001) acknowledged this disparity between the expected structure and the obtained by synthesis due to the difficulty of the entrance of the precursor molecules in the zeolite pores. Meyers et al. used acrylonitrile as the carbon precursor. Nevertheless, in the present work, the formation of pores in the carbon matrix was promoted by heat treatment.

The SEM images obtained between resolutions 0.5–2.0 μm (Fig. 9) also helped to identify the differences in the surfaces of the ZTC due to heat treatment. All the carbons exhibit heterogeneous structures. However, the ZTC obtained at 700 °C (Fig. 9a and b) showed more compact and smoother surfaces, with the development of macropores and mesopores. Pores possibly get formed during the evolution of the volatile matter in the activation process. On the other hand, the carbons obtained at 800 °C (Fig. 9c and d) have a more complex structure with smaller cavities related to micropores and mesopores. Furthermore, there was a change in the morphology of the ZTC 800 A, B, compared to ZTC 700 A, B structures. This discrepancy could be related to thermal stress in the carbons obtained at higher temperature which caused new cracks and holes in the final structure, increasing their porosities (Achaw, 2012).

## 4. Conclusions

Activation of the composite (Z-NaY/heavy crude oil) allowed to obtain mesoporous carbons, however, the microporosities of the Na–Y zeolite were not totally replicated. The use of the surfactant improved the adsorption of the crude oil in the zeolite, obtaining ZTC with higher surface areas (220 ± 3 $m^2/g$) than those obtained using high molecular weight compounds.

The adsorbent materials exhibited average mesoporosities between 4.9 nm and 8.3 nm, with irregular pores shapes. Finally, it is concluded that heavy crude oil, as a mixed model (water-oil system) from an aqueous environment was a starting material suitable for the preparation of “mesoporous” carbons.

The majority of the ZTC previously obtained by CVD (Chemical Vapour Deposition) techniques have a development of microporosity, which enables them to be used in gas adsorption systems. However, in the present work we obtained mesoporous carbons which have the advantage to retain larger molecules, therefore they can be used for the removal of pollutants in water treatment processes like dyes and other organic compounds.

## Conflict of interests

The authors declare that there is not conflict of interest.

## Acknowledgments

We thank the Universidad del Norte and Colciencias for the financial support through doctoral scholarship 2013 (N° UN-OJ-2013-22022), Strategic area “*Biodiversidad, Servicios Ecosistémicos y Bienestar Humano*” (UN-Code 2013-DI0024) and grant program “*Jóvenes Investigadores e Innovadores*” 2012, respectively. Also, we thank to “*Saybolt de Colombia S.A.S.*” for its support with API Gravity analysis and to Ricardo Angulo (RIP) - *Grupo de Procesos Químicos y Bioquímicos Sostenibles (Universidad del Atlántico)*- for his support to the activation process of the composite.

## References

Achaw, O.-W., 2012. A Study of the Porosity of Activated Carbons Using the Scanning Electron Microscope. http://dx.doi.org/10.5772/36337.

Al-Majed, A.A., Adebayo, A.R., Hossain, M.E., 2012. A sustainable approach to controlling oil spills. J. Environ. Manag. 113, 213–227. http://dx.doi.org/10.1016/j.jenvman.2012.07.034.

Al-Qodah, Z., Shawabkah, R., 2009. Production and characterization of granular activated carbon from activated sludge. Braz. J. Chem. Eng. 26, 127–136. http://dx.doi.org/10.1590/S0104-66322009000100012.

ASTM International, 2016. ASTM D2007–11(2016): Standard Test Method for Characteristic Groups in Rubber Extender and Processing Oils and Other Petroleum-derived Oils by the Clay-Gel Absorption Chromatographic Method. ASTM International, West Conshohocken, PA.

ASTM International, 2012. ASTM D1298–12b: Standard Test Method for Density, Relative Density, or API Gravity of Crude Petroleum and Liquid Petroleum Products by Hydrometer Method. ASTM International, West Conshohocken, PA.

Bandura, L., Franus, M., Józefaciuk, G., Franus, W., 2015. Synthetic zeolites from fly ash as effective mineral sorbents for land-based petroleum spills cleanup. Fuel 147, 100–107. http://dx.doi.org/10.1016/j.fuel.2015.01.067.

Bansal, R.C., Goyal, M., 2005. Activated Carbon Adsorption. CRC Press.

Conley, R.T., 1979. Espectroscopia Infrarroja. Madrid etc, Alhambra.

Fukuyama, A.K., Shigenaka, G., Coats, D.A., 2014. Status of intertidal infaunal communities following the Exxon Valdez oil spill in Prince William Sound, Alaska. Mar. Pollut. Bull. 84, 56–69. http://dx.doi.org/10.1016/j.marpolbul.2014.05.043.

Gierszal, K.P., Kim, T.-W., Ryoo, R., Jaroniec, M., 2005. Adsorption and structural properties of ordered mesoporous carbons synthesized by using various carbon precursors and ordered siliceous P6mm and Ia3d mesostructures as templates. J. Phys. Chem. B 109, 23263–23268. http://dx.doi.org/10.1021/jp054562m.

ITOPF, 2015. Oil Tanker Spill Statistics 2015. Int. TANKER Own. Pollut. Fed. http://www.itopf.com/knowledge-resources/data-statistics/statistics/ (Accessed 24 February 2016).

Jin, X., Jiang, M., Shan, X., Pei, Z., Chen, Z., 2008. Adsorption of methylene blue and orange II onto unmodified and surfactant-modified zeolite. J. Colloid Interface Sci. 328, 243–247. http://dx.doi.org/10.1016/j.jcis.2008.08.066.

Jovanovic, M., Grbavcic, Z., Rajic, N., Obradovic, B., 2014. Removal of Cu(II) from aqueous solutions by using fluidized zeolite A beads: hydrodynamic and sorption studies. Chem. Eng. Sci. 117, 85–92. http://dx.doi.org/10.1016/j.ces.2014.06.017.

Karakasi, O.K., Moutsatsou, A., 2010. Surface modification of high calcium fly ash for its application in oil spill clean up. Fuel 89, 3966–3970. http://dx.doi.org/10.1016/j.fuel.2010.06.029.

Kingston, P.F., 2002. Long-term environmental impact of oil spills. Spill Sci. Technol. Bull. 7, 53–61. http://dx.doi.org/10.1016/S1353-2561(02)00051-8.

Kyotani, T., Ma, Z., Tomita, A., 2003. Template synthesis of novel porous carbons using various types of zeolites. Carbon 41, 1451–1459. http://dx.doi.org/10.1016/S0008-6223(03)00090-3.

Kyotani, T., Nagai, T., Inoue, S., Tomita, A., 1997. formation of new type of porous carbon by carbonization in zeolite nanochannels. Chem. Mater 9, 609–615. http://dx.doi.org/10.1021/cm960430h.

Li, G., 2005. Ft-IR Studies of Zeolite Materials: Characterization and Environmental Applications. Theses Diss.

Li, Q., Qi, Y., Gao, C., 2015. Chemical regeneration of spent powdered activated carbon used in decolorization of sodium salicylate for the pharmaceutical industry. J. Clean. Prod. 86, 424–431. http://dx.doi.org/10.1016/j.jclepro.2014.08.008.

Liu, D., Zhu, L., 2014. Assessing China's legislation on compensation for marine ecological damage: a case study of the Bohai oil spill. Mar. Policy 50 (Part A), 18–26. http://dx.doi.org/10.1016/j.marpol.2014.05.009.

Ma, Z., Kyotani, T., Tomita, A., 2002. Synthesis methods for preparing microporous carbons with a structural regularity of zeolite Y. Carbon 40, 2367–2374. http://dx.doi.org/10.1016/S0008-6223(02)00120-3.

Marsh, H., Rodríguez-Reinoso, F., 2006. Activated Carbon. Elsevier.

Meyers, C.J., Shah, S.D., Patel, S.C., Sneeringer, R.M., Bessel, C.A., Dollahon, N.R., Leising, R.A., Takeuchi, E.S., 2001. Templated synthesis of carbon materials from zeolites (Y, beta, and ZSM-5) and a montmorillonite clay (K10): physical and electrochemical characterization. J. Phys. Chem. B 105, 2143–2152. http://dx.doi.org/10.1021/jp0029663.

MINAMBIENTE, 2015. Si terminamos el conflicto, los dividendos para el medio ambiente serán inmensos: Presidente Santos | Ministerio de Ambiente y Desarrollo Sostenible. https://www.minambiente.gov.co/index.php/component/content/article/122-noticias-minambiente/2149-si-terminamos-el-conflicto-los-dividendos-para-el-medio-ambiente-seran-inmensos-presidente-santos (Accessed 29 February 2016).

Mohanty, K., Jha, M., Meikap, B.C., Biswas, M.N., 2005. Removal of chromium (VI) from dilute aqueous solutions by activated carbon developed from Terminalia arjuna nuts activated with zinc chloride. Chem. Eng. Sci. 60, 3049–3059. http://dx.doi.org/10.1016/j.ces.2004.12.049.

Powder Diffraction File-2 (PDF-2), International Centre for Diffraction Data (ICDD), 12 Campus Blvd., Newtown Square PA 19073–3273, U.S.A., n.d.

Radovic, L.R., 2007. Chemistry & Physics of Carbon. CRC Press.

Raj, K.G., Joy, P.A., 2015. Coconut shell based activated carbon–iron oxide magnetic nanocomposite for fast and efficient removal of oil spills. J. Environ. Chem. Eng. 3, 2068–2075. http://dx.doi.org/10.1016/j.jece.2015.04.028.

Riehm, D.A., Neilsen, J.E., Bothun, G.D., John, V.T., Raghavan, S.R., McCormick, A.V., 2015. Efficient dispersion of crude oil by blends of food-grade surfactants: toward greener oil-spill treatments. Mar. Pollut. Bull. 101, 92–97. http://dx.doi.org/10.1016/j.marpolbul.2015.11.012.

Ron, E.Z., Rosenberg, E., 2014. Enhanced bioremediation of oil spills in the sea. Curr. Opin. Biotechnol. Energy Biotechnol. Environ. Biotechnol. 27, 191–194. http://dx.doi.org/10.1016/j.copbio.2014.02.004.

Sakthivel, T., Reid, D.L., Goldstein, I., Hench, L., Seal, S., 2013. Hydrophobic high surface area zeolites derived from fly ash for oil spill remediation. Environ. Sci. Technol. 47, 5843–5850. http://dx.doi.org/10.1021/es3048174.

Sang, S., Liu, Z., Tian, P., Liu, Z., Qu, L., Zhang, Y., 2006. Synthesis of small crystals zeolite NaY. Mater. Lett. 60, 1131–1133. http://dx.doi.org/10.1016/j.matlet.2005.10.110.

Speight, J.G., 2014. The Chemistry and Technology of Petroleum, fifth ed. CRC Press.

Su, F., Zhao, X.S., Lv, L., Zhou, Z., 2004. Synthesis and characterization of microporous carbons templated by ammonium-form zeolite Y. Carbon 42, 2821–2831. http://dx.doi.org/10.1016/j.carbon.2004.06.028.

Tansel, B., Regula, J., Shalewitz, R., 1995. Treatment of fuel oil and crude oil contaminated waters by ultrafiltration membranes. Desalination. In: Proceedings of the American Desalting Association 1994 Biennial Conference and Exposition Membrane and Desalting Technologies, vol. 102, pp. 301–311. http://dx.doi.org/10.1016/0011-9164(95)00067-C.

Thommes, M., Kaneko, K., Neimark, A.V., Olivier, J.P., Rodriguez-Reinoso, F., Rouquerol, J., Sing, K.S.W., 2015. Physisorption of gases, with special reference to the evaluation of surface area and pore size distribution (IUPAC Technical Report). Pure Appl. Chem. 87, 1051–1069. http://dx.doi.org/10.1515/pac-2014-1117.

Tiwari, P., Deo, M., 2012. Compositional and kinetic analysis of oil shale pyrolysis using TGA–MS. Fuel 94, 333–341. http://dx.doi.org/10.1016/j.fuel.2011.09.018.

US. Energy Information Administration, 2016. Short-term Energy Outlook - U.S. Energy Information Administration (EIA). https://www.eia.gov/forecasts/steo/report/global_oil.cfm (Accessed 14 March 2016).

Vidal, C.B., Raulino, G.S.C., Barros, A.L., Lima, A.C.A., Ribeiro, J.P., Pires, M.J.R., Nascimento, R.F., 2012. BTEX removal from aqueous solutions by HDTMA-modified Y zeolite. J. Environ. Manag. 112, 178–185. http://dx.doi.org/10.1016/j.jenvman.2012.07.026.

Wei, C.-L., Rowe, G.T., Escobar-Briones, E., Nunnally, C., Soliman, Y., Ellis, N., 2012. Standing stocks and body size of deep-sea macrofauna: predicting the baseline of 2010 Deepwater Horizon oil spill in the northern Gulf of Mexico. Deep Sea Res. Part Oceanogr. Res. Pap. 69, 82–99. http://dx.doi.org/10.1016/j.dsr.2012.07.008.

Zeolyst, n.d. Zeolite Y [WWW Document]. URL http://www.zeolyst.com/our-products/standard-zeolite-powders/zeolite-y.aspx (Accessed 15 March 2016).